Defence Research and Development Canada
Recherche et développement pour la défense Canada

DEFENCE R&D DÉFENSE

Modification of a high frequency radar echo spatial correlation function by propagation in a linear plasma density profile

Ryan J. Riddolls

Defence R&D Canada – Ottawa

Technical Memorandum
DRDC Ottawa TM 2011-219
December 2011

Canada

Modification of a high frequency radar echo spatial correlation function by propagation in a linear plasma density profile

Ryan J. Riddolls
Defence R&D Canada – Ottawa

Defence R&D Canada – Ottawa
Technical Memorandum
DRDC Ottawa TM 2011-219
December 2011

Principal Author

Original signed by R. J. Riddolls

R. J. Riddolls

Approved by

Original signed by C. Gierull

C. Gierull
Acting Head/Radar Systems Section

Approved for release by

Original signed by C. McMillan

C. McMillan
Head/Document Review Panel

Abstract

This memorandum examines the spatial autocorrelation function for echoes from an ionospheric plasma in the High Frequency (HF) range. Conventional treatments of this problem assume that the amount of signal phase shift for a given plasma density fluctuation in the ionospheric propagation medium remains constant along the propagation path. For HF radar signal propagation through an ionospheric plasma with field-aligned density structures, the spatial phase autocorrelation is predicted to be highly anisotropic, with essentially perfect correlation in the magnetic north-south direction. In this memorandum a revised theory is provided that accounts for a spatial-dependent derivative of signal wavenumber with respect to plasma density in an ionosphere with a linear plasma density profile. This revised theory leads to a prediction of a far more isotropic autocorrelation, with an axial ratio equal to the cosecant of the local magnetic dip angle. This theory provides a more realistic basis for predicting the performance of spatial adaptive antenna arrays for the rejection of vertical incidence ionospheric clutter in HF Surface Wave Radar (HFSWR) systems.

Résumé

Dans le présent mémoire, on examine une fonction d'autocorrélation spatiale pour les échos d'un plasma ionosphérique dans la gamme des hautes fréquences (HF). Les méthodes classiques utilisées pour traiter ce problème reposent sur l'hypothèse que la quantité de déphasage de signal pour une certaine fluctuation de la densité de plasma dans un milieu de propagation ionosphérique demeure constante le long du trajet de propagation. On s'attend à une phase d'autocorrélation hautement anisotrope, ainsi qu'à une corrélation essentiellement parfaite dans la direction magnétique nord-sud, dans le cas d'une propagation des signaux radar HF dans un plasma ionosphérique dont les structures de densité sont alignées sur les champs. Dans le mémoire, on présente une théorie révisée qui tient compte d'une dérivée dépendante de l'espace qui concerne le nombre d'ondes de signaux et se rapporte à la densité de plasma dans une ionosphère à profil de densité de plasma linéaire. La théorie révisée donne lieu à la prévision d'une autocorrélation encore plus isotrope, dont le rapport axial équivaut à la cosécante de l'angle d'inclinaison magnétique local. Cette théorie constitue une base plus réaliste pour prévoir le rendement d'antennes réseau spatiales adaptatives quant au rejet de clutter ionosphérique dans les systèmes de radar haute fréquence à ondes de surface (RHFOS).

This page intentionally left blank.

Executive summary

Modification of a high frequency radar echo spatial correlation function by propagation in a linear plasma density profile

Ryan J. Riddolls; DRDC Ottawa TM 2011-219; Defence R&D Canada – Ottawa; December 2011.

Background: High Frequency Surface Wave Radar (HFSWR) is a technology that uses the propagation of waves along the surface of the ocean to detect ships at ranges of a few hundred kilometres. However, these radars also emit small amounts of radiation in the vertical direction, leading to radar clutter comprising echoes from the earth's ionosphere. Because the surface targets and the ionosphere are at similar ranges, targets can become masked by clutter. This problem has led to the design of adaptive antenna arrays that can suppress signals coming from overhead of the array while maintaining response to signals arriving from the horizon. Good performance of the adaptive antenna array depends on the ionospheric reflections having good correlation properties over the area of the antenna array, so that the reflections can be accurately subtracted from the radar data. The departure from perfect correlation is captured in the signal autocorrelation function. Conventional calculations of the autocorrelation function predict a highly anisotropic situation, consisting of essentially perfect correlation in the magnetic north-south direction, and a decreasing correlation with horizontal distance in the magnetic east-west direction. However, this highly anisotropic situation is not seen in practice.

Results: A new theory is developed that accounts for the variation in the amount of signal phase caused by a given fluctuation of plasma density as a signal propagates through the ionosphere, leading to the prediction of a much more isotropic autocorrelation function, with an axial ratio equal to the cosecant of the magnetic dip angle. This result is compatible with observations from ionospheric clutter experiments.

Significance: This theory provides a more realistic basis for predicting the performance of spatial adaptive antenna arrays for the rejection of ionospheric clutter in HFSWR systems. The radar designer can determine the best adaptive array configurations without the need for an experimental cycle. The radar analyst can also determine the performance gained by inserting the technology into existing systems.

Future Work: The theory could be extended to the case of oblique (non-vertical incidence) propagation, although the mathematics would be more complicated since the radar pulse trajectory is no longer rotationally symmetric around a vertical axis. This extension would allow for the analysis of mixed sky-surface propagation paths.

Sommaire

Modification of a high frequency radar echo spatial correlation function by propagation in a linear plasma density profile

Ryan J. Riddolls; DRDC Ottawa TM 2011-219; R & D pour la défense Canada – Ottawa; décembre 2011.

Contexte : Les systèmes de radar haute fréquence à ondes de surface (RHFOS) exploitent la propagation des ondes sur la surface de l'eau salée conductrice de l'océan pour détecter des navires, à des portées de quelques centaines de kilomètres. Toutefois, ces radars émettent également de petites quantités de rayonnement vertical qui génèrent du fouillis radar composé, entre autres, des échos de l'ionosphère de la Terre. Les cibles de surface peuvent être masquées par ce fouillis, puisqu'elles sont à une même portée que l'ionosphère. En vue de résoudre ce problème, on a conçu des antennes réseau adaptatives qui peuvent neutraliser les signaux au-dessus du réseau tout en maintenant une réponse à ceux provenant de l'horizon. Le rendement de ces antennes, et donc l'exactitude avec laquelle les réflexions peuvent être retirées des données radar, dépend des propriétés de corrélation des réflexions ionosphériques dans la zone au-dessus de l'antenne réseau. La fonction d'autocorrélation du signal témoigne de l'écart par rapport à la corrélation parfaite. En théorie, selon les calculs classiques de la fonction d'autocorrélation, on prévoit une situation hautement anisotrope qui consiste en une corrélation essentiellement parfaite dans la direction magnétique nord-sud et en une corrélation décroissante selon la distance horizontale dans la direction magnétique est-ouest. En pratique, toutefois, cette situation hautement anisotrope n'est pas survenue.

Résultats : On a élaboré une nouvelle théorie qui prend en compte les variations de la quantité de signaux en phase causées par une fluctuation donnée de la densité de plasma pendant la propagation d'un signal dans l'ionosphère, ce qui a mène à la prévision d'une fonction d'autocorrélation beaucoup plus isotrope, dont le rapport axial correspond à la cosécante de l'angle d'inclinaison magnétique. Cette prévision est compatible avec les observations faites au cours d'autres expériences en matière de fouillis ionosphérique.

Portée : Cette théorie constitue une base plus réaliste pour prévoir le rendement d'antennes réseau spatiales adaptatives quant au rejet de fouillis ionosphérique dans les systèmes de RHFOS. Le concepteur du radar peut déterminer les meilleures configurations d'antenne réseau adaptative, sans avoir recours à un cycle d'expériences. L'analyste radar, quant à lui, peut déterminer le rendement obtenu lors de l'intégration de la technologie à des systèmes existants.

Recherches futures : On pourrait appliquer cette théorie à la propagation oblique (incidence non verticale), ce qui permettrait d'analyser des trajets de propagation touchant des surfaces ionosphérique mixtes. Toutefois, des calculs plus complexes seraient nécessaires, puisque la trajectoire de l'impulsion radar ne décrit plus une rotation symétrique autour d'un axe vertical.

This page intentionally left blank.

Table of contents

This page intentionally left blank.

1 Introduction

High Frequency Surface Wave Radar (HFSWR) is a technology that uses the propagation of waves along the surface of the electrically conducting salt water ocean to illuminate beyond-the-horizon ocean vessel targets [1]. To achieve sufficiently low attenuation to allow target detection capability to a few hundred kilometres, the radar has to operate in the range of frequencies below 10 MHz. However, signals in this frequency range reflect from the earth's ionosphere [2]. The transmit and receive antennas available to HFSWR systems do not have perfect overhead nulls, and thus clutter comprising vertical incidence ionospheric reflections can mask target echoes.

Spatial adaptive signal processing using two-dimensional arrays can be used to suppress ionospheric clutter arising from vertical incidence propagation [3, 4]. The degree of suppression is related to the autocorrelation of the signal complex amplitude in the horizontal plane. There are several ways to determine the spatial autocorrelation of signals reflected from the ionosphere. These methods generally involve computing the signal phase as a deterministic function of an arbitrary realization of plasma density structure along the signal path. The density structure can be either discrete [5] or continuous [6]. This deterministic function can then be used to relate the spatial power spectrum of the plasma density structure to the spatial power spectrum of the signal phase [7]. The inverse Fourier transform is then applied to the spatial power spectrum to compute the autocorrelation. Finally, the phase autocorrelation is used to compute the complex amplitude autocorrelation.

In conventional theories of the two-dimensional autocorrelation function for ionospherically propagated signals, the autocorrelation function is found to be highly anisotropic in the horizontal plane [8]. The predicted echoes are essentially perfectly correlated in the magnetic north-south direction, although such ideal behaviour is not seen in experiments [4]. There has been interest in finding a simple explanation for the lack of anisotropy in the received signal autocorrelation. It is shown in this memorandum that a proper accounting of the derivative of radar signal wavenumber with respect to local plasma density can provide an adequate explanation for the lack of observed anisotropy.

The exposition of the signal autocorrelation is carried out in the next three chapters. Chapter 2 derives phase as a function of the plasma density structure along the propagation path and relates the power spectrum of the phase to the power spectrum of the plasma density. Chapter 3 adopts a model for the power spectrum of the plasma density, computes the signal phase autocorrelation via a two-dimensional inverse Fourier transform, and converts the phase autocorrelation function into the complex amplitude autocorrelation function. A short conclusion with some discussion is provided in Chapter 4.

2 Derivation of the phase spectrum

In this chapter we derive the phase spatial spectrum for ionospheric echoes observed by HFSWR systems, incorporating effects that are not normally accounted for in conventional treatments of ionospheric propagation, as discussed in Chapter 1. We will compare the derived results with those of conventional treatments.

2.1 Phase fluctuations

We consider an unmagnetized model of the ionosphere such that the dispersion relation for the propagating radar signal is [9]

$$N^2 = \frac{c^2 k^2}{\omega^2} = 1 - \frac{\omega_p^2}{\omega^2}, \tag{1}$$

where N is the index of refraction, c is the speed of light, $k = |\mathbf{k}|$ is the wavenumber, ω is the frequency, and ω_p is the electron plasma frequency, defined as

$$\omega_p^2 = \frac{e^2 n}{\epsilon_0 m}, \tag{2}$$

where e is the charge on an electron, n is the density of plasma in electrons per unit volume, ϵ_0 is the permittivity of free space, and m is the mass of an electron.

In the ionosphere, n is a function of space. Let us consider a system of cartesian coordinates with x east, y north, and z vertical. The simplest space-dependent model of the ionosphere assumes that n is linearly related to altitude z, slowly varying compared to the radar wavelength, and independent of the horizontal coordinate. Using (2), we can write a z-dependent plasma frequency:

$$\omega_p^2(z) = \omega^2 \frac{z}{z_0}. \tag{3}$$

Here, $z = 0$ is the bottom of the ionosphere and $z = z_0$ is the height of the reflection (about 50 km above the bottom of the ionosphere). Assume that a radar signal is launched from the ground with wavenumber $\mathbf{k} = k\hat{\mathbf{z}}$, where $\hat{\mathbf{z}}$ is a unit vector in the vertical direction. In a plane-stratified ionosphere where n is only a function of z, it follows from (1) and (2) that N also depends only on z. By Snell's law, the x and y components of the wavenumber $\mathbf{k}$ remain exactly zero as the radar pulse propagates through the ionosphere. Furthermore, since the plasma model is unmagnetized in this treatment, the direction of propagation is equal to the local wavenumber $\mathbf{k}$ [2]. Thus, the radar signal wave packet travels vertically up, reflects from the ionosphere, and travels vertically down along the same path. The total phase accrued during propagation in the ionosphere is

$$\phi = 2 \int_0^{z_0} k(z)\, dz. \tag{4}$$

Consider small-amplitude irregularities in the ionospheric plasma, such that the total ionospheric plasma density is $n = n_0 + n_1$, where n_0 is the background plasma density and n_1 is the irregularity. The first-order Taylor series perturbation to ϕ is given by

$$\phi_1 = 2 \int_0^{z_0} n_1(x, y, z) \frac{\partial k(z)}{\partial n} \, dz. \tag{5}$$

From (1), (2), and (3) we can compute the derivative of k with respect to density:

$$\frac{\partial k(z)}{\partial n} = -\frac{e^2}{2\epsilon_0 m \omega c \sqrt{1 - \omega_p^2/\omega^2}} = -\frac{r_e \lambda}{\sqrt{1 - z/z_0}}, \tag{6}$$

where $r_e = e^2/(4\pi\epsilon_0 m c^2)$ is the classical electron radius (2.8×10^{-15} m) and λ is the free space radar wavelength. The expression for the phase fluctuation, accounting for $\partial k/\partial n$, is

$$\phi_1 = -2 r_e \lambda \int_0^{z_0} \frac{n_1(x, y, z) \, dz}{\sqrt{1 - z/z_0}}. \tag{7}$$

We propose a slight modification to this expression. The root-mean square (RMS) amplitude of the density fluctuation n_1 varies with height. A common assumption is that the RMS amplitude of the fractional fluctuation n_1/n is constant [10], which means that the RMS amplitude of n_1 is proportional to z. We explicitly write out this dependence, so that n_1 represents the size of the fluctuation at $z = z_0$:

$$n_1(x, y, z) \longrightarrow n_1(x, y, z) \frac{z}{z_0}. \tag{8}$$

The final expression for the phase fluctuation is therefore

$$\phi_1 = -2 r_e \lambda \int_0^{z_0} \frac{n_1(x, y, z)(z/z_0) \, dz}{\sqrt{1 - z/z_0}}. \tag{9}$$

Before proceeding, we emphasize that we have captured two additional effects compared to conventional modelling of ionospheric irregularities. The major effect is the rapid increase in $\partial k/\partial n$ as one approaches the reflection height at $z = z_0$, due to the denominator in the integrand above. An additional minor effect is the linear increase in the RMS amplitude of the fluctuation n_1 with height, appearing as the (z/z_0) factor in the numerator of the integrand. Conventional treatments ignore both effects and generally work with the simpler expression [8]:

$$\phi_1 = -2 r_e \lambda \int_0^{z_0} n_1(x, y, z) \, dz. \tag{10}$$

2.2 Phase spectrum

For ground-based radar spatial adaptive beamforming applications, we are interested in the autocorrelation of the phase in the x (east) and y (north) directions:

$$R_{\phi_1}(X,Y) = \langle \phi_1(x+X, y+Y)\phi_1^*(x,y) \rangle \,, \tag{11}$$

where X and Y are the lags in the x and y directions, respectively. In this expression, $\phi_1(x,y)$ refers to the phase perturbation accrued in the ionosphere above a location (x,y) on the ground. Combining (9) and (11), we have

$$R_{\phi_1}(X,Y) = 4(r_e\lambda)^2 \int_0^{z_0}\int_0^{z_0} \frac{R_{n_1}(X,Y,z-z')(zz'/z_0^2)}{\sqrt{(1-z/z_0)(1-z'/z_0)}}\, dz\, dz', \tag{12}$$

where $R_{n_1}(X,Y,Z)$ is the spatial autocorrelation of n_1. To make R_{n_1} a function of only one variable, we perform the following transformation:

$$u = (z-z')/z_0 \tag{13}$$

$$v = (z+z')/z_0. \tag{14}$$

The Jacobian determinant is

$$J(u,v) = \left| \begin{array}{cc} \dfrac{\partial z}{\partial u} & \dfrac{\partial z'}{\partial u} \\ \dfrac{\partial z}{\partial v} & \dfrac{\partial z'}{\partial v} \end{array} \right| = \frac{z_0^2}{2}. \tag{15}$$

The region of integration in the new (u,v) coordinates is a square with vertices at (0,0), (1,1), (0,2), and (-1,1), hence

$$R_{\phi_1}(X,Y) = (r_e\lambda z_0)^2 \int_{-1}^{1} R_{n_1}(X,Y,z_0u) \left[\int_{|u|}^{-|u|+2} \frac{(v^2-u^2)\, dv}{\sqrt{(v-2)^2-u^2}} \right] du. \tag{16}$$

$$= (r_e\lambda z_0)^2 \int_{-1}^{1} R_{n_1}(X,Y,z_0u) \left\{ \int_{|u|}^{-|u|+2} \frac{[(v-2)^2-u^2]\, dv}{\sqrt{v^2-u^2}} \right\} du. \tag{17}$$

The following indefinite integral can be verified by differentiation:

$$\int \frac{[(v-2)^2-u^2]\, dv}{\sqrt{v^2-u^2}} = \frac{v-8}{2}\sqrt{v^2-u^2} - \frac{u^2-8}{2} \log\left(\sqrt{v^2-u^2}+v\right). \tag{18}$$

The definite integral becomes

$$\int_{|u|}^{-|u|+2} \frac{[(v-2)^2-u^2]\, dv}{\sqrt{v^2-u^2}}$$

$$= -\frac{|u|+6}{2}\sqrt{(|u|-2)^2-u^2} - \frac{u^2-8}{2} \log\left(\frac{2\sqrt{1-|u|}-|u|+2}{|u|} \right). \tag{19}$$

Since the correlation length associated with R_{ϕ_1} is small compared to z_0, the only significant contribution to the integral over u occurs for $|u| \ll 1$, therefore

$$\lim_{u\to 0} \int_{|u|}^{-|u|+2} \frac{[(v-2)^2 - u^2]\, dv}{\sqrt{v^2-u^2}} \approx 4\log\left(\frac{4}{|u|}\right) - 6 \approx 4\log\left(\frac{1}{|u|}\right). \tag{20}$$

We can insert this result into the expression (17) for the autocorrelation:

$$R_{\phi_1}(X,Y) = 4(r_e\lambda z_0)^2 \int_{-1}^{1} R_{n_1}(X,Y,z_0u)\log\left(\frac{1}{|u|}\right)\, du \tag{21}$$

$$= 4z_0(r_e\lambda)^2 \int_{-\infty}^{\infty} R_{n_1}(X,Y,Z)\log\left(\frac{z_0}{|Z|}\right)\mu(z_0-|Z|)\, dZ, \tag{22}$$

where μ is the unit step function. However, typically R_{n_1} is of a complicated form that precludes direct evaluation of the above integral. An alternate way to calculate the integral uses Fourier transforms. Taking Fourier transforms of both sides yields

$$S_{\phi_1}(\kappa_x,\kappa_y) = 4z_0(r_e\lambda)^2$$
$$\times \int_{-\infty}^{\infty}\int_{-\infty}^{\infty}\int_{-\infty}^{\infty} R_{n_1}(X,Y,Z)\log\left(\frac{z_0}{|Z|}\right)\mu(z_0-|Z|)e^{-i\kappa_x X - i\kappa_y Y}\, dX dY dZ. \tag{23}$$

The transforms along the X and Y axes are straightforward. We can also interpret the integral over Z as a Fourier transform if we evaluate the resulting transform at $\kappa_z = 0$. Furthermore, using the convolution theorem, we can separate the plasma density spectrum from the logarithm and unit step functions as follows:

$$S_{\phi_1}(\kappa_x,\kappa_y) = 4z_0(r_e\lambda)^2 \left\{ \frac{1}{2\pi} S_{n_1}(\kappa_x,\kappa_y,\kappa_z) \overset{\kappa_z}{*} \mathcal{F}\left[\log\left(\frac{z_0}{|Z|}\right)\mu(z_0-|Z|)\right]\right\}_{\kappa_z=0}, \tag{24}$$

where $\mathcal{F}$ denotes a Fourier transform and $\overset{\kappa_z}{*}$ denotes a convolution with respect to the κ_z coordinate. The required Fourier transform is

$$\mathcal{F}\left[\log\left(\frac{z_0}{|Z|}\right)\mu(z_0-|Z|)\right] = \frac{2\mathrm{Si}(\kappa_z z_0)}{\kappa_z}, \tag{25}$$

where $\mathrm{Si}(x)$ is the sine integral:

$$\mathrm{Si}(x) = \int_0^x \frac{\sin t}{t}\, dt. \tag{26}$$

The above Fourier transform can be proven by recognizing the symmetry of the argument and then using the method of integration by parts. For the convenience of

the reader, a derivation of the transform is provided as follows:

$$\mathcal{F}\left[\log\left(\frac{z_0}{|Z|}\right)\mu(z_0-|Z|)\right] = \int_{-\infty}^{\infty}\log\left(\frac{z_0}{|Z|}\right)\mu(z_0-|Z|)e^{-ik_zZ}\,dZ \tag{27}$$

$$= -2\int_0^{z_0}\log\left(\frac{Z}{z_0}\right)\cos(k_zZ)\,dZ \tag{28}$$

$$= -2\log\left(\frac{Z}{z_0}\right)\frac{\sin(k_zZ)}{k_z}\bigg|_0^{z_0} + 2\int_0^{z_0}\frac{\sin(k_zZ)}{k_zZ}\,dZ. \tag{29}$$

The first term on the right side evaluates to zero. Setting $t = k_zZ$, we find that

$$\mathcal{F}\left[\log\left(\frac{z_0}{|Z|}\right)\mu(z_0-|Z|)\right] = \frac{2}{k_z}\int_0^{k_zz_0}\frac{\sin t}{t}\,dt \tag{30}$$

$$= \frac{2\mathrm{Si}(k_zz_0)}{k_z}, \tag{31}$$

as was required to be shown.

We emphasize here that the additional effect being captured in this model is the convolution of $S_{n_1}(\kappa_x,\kappa_y,\kappa_z)$ with the sine integral in (24). Conventional modelling of ionospheric irregularities ignores this effect, and uses the expression [8]

$$S_{\phi_1}(\kappa_x,\kappa_y) = 4z_0(r_e\lambda)^2 S_{n_1}(\kappa_x,\kappa_y,\kappa_z)\Big|_{\kappa_z=0}. \tag{32}$$

In the next chapter, we invoke an explicit expression for $S_{n_1}(\kappa_x,\kappa_y,\kappa_z)$ to find the phase spectrum $S_{\phi_1}(\kappa_x,\kappa_y)$, the phase autocorrelation $R_{\phi_1}(\kappa_x,\kappa_y)$ and ultimately the complex amplitude autocorrelation.

3 Derivation of the phase autocorrelation

The performance of radar adaptive signal processing algorithms often depends on the signal autocorrelation function [4]. This motivates the derivation in this chapter. We invoke a specific expression for the plasma density spectrum, which allows one to complete the inverse Fourier transform of the phase spectrum (24) in order to find the phase autocorrelation.

3.1 Plasma density spectrum

To get an explicit expression for the phase fluctuation spectrum, we need to determine the plasma density fluctuation spectrum. For S_{n_1}, we adopt a very simple third-order spatial power spectrum for infinitely-extended field-aligned plasma irregularties [11, 12]:

$$S_{n_1}(\boldsymbol{\kappa}) = \frac{4\pi^2\kappa_0 \left\langle n_1^2 \right\rangle \delta(\kappa_\parallel)}{(\kappa_0^2 + \kappa_\perp^2)^{3/2}}, \tag{33}$$

where κ_0 is the "outer" scale length parameter, $\kappa_\perp$ is the magnitude of the component of the density irregularity wavenumber $\mathbf{k}$ that is perpendicular to the earth's magnetic field, $\kappa_\parallel$ is the magnitude of the component of $\mathbf{k}$ along the field, $\langle n_1^2 \rangle$ is the mean-square plasma density fluctuation at $z = z_0$, and the spectrum is normalized such that

$$\left\langle n_1^2 \right\rangle = \frac{1}{(2\pi)^3} \int S_{n_1}(\kappa_x, \kappa_y, \kappa_z)\, d\kappa_x d\kappa_y d\kappa_z. \tag{34}$$

We suppose that the magnetic field of the earth follows a unit vector $\hat{\mathbf{l}} = (l_x, l_y, l_z)$. However, wave propagation is strictly along the z direction. Without loss of generality, we can rotate the x and y axes around the z axis such that the magnetic field vector lies in the yz plane and $l_x = 0$. The quantity $\kappa_\parallel$ is given by the dot product of $\boldsymbol{\kappa}$ and $\hat{\mathbf{l}}$, which under the assumption of $l_x = 0$ is given by

$$\kappa_\parallel = \kappa_y l_y + \kappa_z l_z, \tag{35}$$

whereas $\kappa_\perp$ takes the following form:

$$\kappa_\perp^2 = \kappa_x^2 + \kappa_y^2 + \kappa_z^2 - \kappa_\parallel^2 = \kappa_x^2 + (\kappa_y l_z - \kappa_z l_y)^2, \tag{36}$$

where we have used the relation $l_y^2 + l_z^2 = 1$. In light of these definitions, the phase spectrum in cartesian coordinates is

$$S_{n_1}(\kappa_x, \kappa_y, \kappa_z) = \frac{4\pi^2\kappa_0 \left\langle n_1^2 \right\rangle \delta(\kappa_y l_y + \kappa_z l_z)}{[\kappa_0^2 + \kappa_x^2 + (\kappa_y l_z - \kappa_z l_y)^2]^{3/2}}. \tag{37}$$

This expression can now be inserted into (24) to arrive at an explicit form of $S_{\phi_1}(\kappa_x, \kappa_y)$, which permits inverse Fourier transformation.

3.2 Phase autocorrelation

We can now compute the convolution in (24). The convolution can be written as:

$$S_{\phi_1}(\kappa_x,\kappa_y) = 16\pi\kappa_0 z_0 (r_e\lambda)^2 \left\langle n_1^2 \right\rangle \int_{-\infty}^{\infty} \frac{\mathrm{Si}(\kappa_z z_0)\delta(\kappa_y l_y + \kappa_z l_z)\, d\kappa_z}{\kappa_z[\kappa_0^2 + \kappa_x^2 + (\kappa_y l_z - \kappa_z l_y)^2]^{3/2}} \tag{38}$$

$$= \frac{16\pi\kappa_0 z_0 (r_e\lambda)^2 \left\langle n_1^2 \right\rangle \mathrm{Si}(\kappa_y l_y z_0/l_z)}{\kappa_y l_y(\kappa_0^2 + \kappa_x^2 + \kappa_y^2/l_z^2)^{3/2}}. \tag{39}$$

The correlation function $R_{\phi_1}(X,Y)$ is found by applying the inverse Fourier transform to (39) with respect to κ_x and κ_y. The inverse transform over κ_x uses (9.6.25) in [13]:

$$R_{\phi_1}(X,Y) = \frac{1}{(2\pi)^2}\int_{-\infty}^{\infty}\int_{-\infty}^{\infty} \frac{16\pi\kappa_0 z_0 (r_e\lambda)^2 \left\langle n_1^2 \right\rangle \mathrm{Si}(\kappa_y l_y z_0/l_z) e^{i\kappa_x X + i\kappa_y Y}\, d\kappa_x\, d\kappa_y}{\kappa_y l_y(\kappa_0^2 + \kappa_x^2 + \kappa_y^2/l_z^2)^{3/2}} \tag{40}$$

$$= \int_{-\infty}^{\infty} \frac{8\kappa_0 z_0 (r_e\lambda)^2 \left\langle n_1^2 \right\rangle \mathrm{Si}(\kappa_y l_y z_0/l_z)|X| K_1[(\kappa_0^2 + \kappa_y^2/l_z^2)^{1/2}|X|] e^{i\kappa_y Y}\, d\kappa_y}{\pi\kappa_y l_y(\kappa_0^2 + \kappa_y^2/l_z^2)^{1/2}}, \tag{41}$$

where K_1 is the first-order modified Bessel function of the second kind. The integral over κ_y is more complicated. We consider the condition $|X| \ll \kappa_0^{-1}$, such that

$$1 \approx (\kappa_0^2 + \kappa_y^2/l_z^2)^{1/2}|X| K_1[(\kappa_0^2 + \kappa_y^2/l_z^2)^{1/2}|X|] \equiv f(\kappa_y), \tag{42}$$

while the rest of the integrand varies rapidly and acts as a Dirac delta function. The integral evaluates to $f(0)$ multiplied by the area of the delta function:

$$R_{\phi_1}(X,Y)\Big|_{|X| \ll \kappa_0^{-1}} = \kappa_0|X|K_1(\kappa_0|X|)\int_{-\infty}^{\infty} \frac{8\kappa_0 z_0 (r_e\lambda)^2 \left\langle n_1^2 \right\rangle \mathrm{Si}(\kappa_y l_y z_0/l_z) e^{i\kappa_y Y}\, d\kappa_y}{\pi\kappa_y l_y(\kappa_0^2 + \kappa_y^2/l_z^2)}. \tag{43}$$

Under the conditions $|Y| \ll \kappa_0^{-1}$ and $|Y| \ll z_0$, the exponential is approximately unity when κ_y is on the order of κ_0 or z_0^{-1}, which are the integrand breakpoints. The value of the integral therefore only depends on the high-frequency asymptote of the integrand and the area under the integrand function. This permits the approximation

$$\frac{\mathrm{Si}(x)}{x} \approx \frac{\pi/2}{\sqrt{(\pi/2)^2 + x^2}}. \tag{44}$$

This approximation preserves the high frequency ($x \gg 1$) asymptote and numerical integration will show the area is preserved to within 7%. We insert (44) into (43):

$$R_{\phi_1}(X,Y)\Big|_{\substack{|X| \ll \kappa_0^{-1} \\ |Y| \ll \kappa_0^{-1}, z_0}} = \kappa_0|X|K_1(\kappa_0|X|)\int_{-\infty}^{\infty} \frac{4\kappa_0 z_0 (r_e\lambda)^2 \left\langle n_1^2 \right\rangle e^{i\kappa_y Y}\, d\kappa_y}{l_y l_z[\pi^2/(2z_0 l_y)^2 + \kappa_y^2/l_z^2]^{1/2}(\kappa_0^2 + \kappa_y^2/l_z^2)}. \tag{45}$$

Unfortunately, this integral cannot be evaluated in closed form. However, one can show $\kappa_0^2 \approx \pi^2/(2z_0 l_y)^2$, such that the two bracketed factors in the denominator can combine into a single factor.

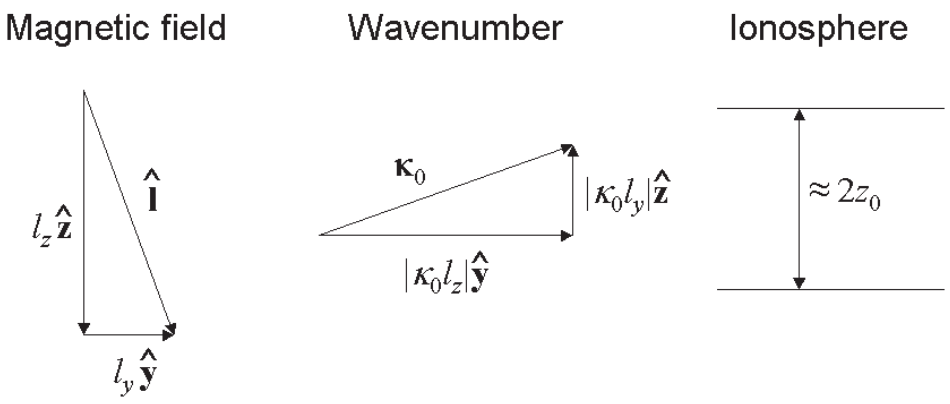

Figure 1: *Relation of κ_0 to the ionospheric profile.*

The parameter κ_0 in (33) is the minimum plasma density wavenumber supported by the ionosphere, perpendicular to the magnetic field. In Figure 1, the magnetic field is shown as vector $\hat{\mathbf{l}} = l_y\hat{\mathbf{y}} + l_z\hat{\mathbf{z}}$, where $\hat{\mathbf{y}}$ and $\hat{\mathbf{z}}$ are unit vectors in the horizontal and vertical directions, respectively. We visualize κ_0 as the magnitude of a vector $\boldsymbol{\kappa_0}$ perpendicular to the magnetic field, with horizontal component $|\kappa_0 l_z|\hat{\mathbf{y}}$ and vertical component $|\kappa_0 l_y|\hat{\mathbf{z}}$. We take the thickness of the ionosphere to be on the order of $2z_0$, assuming that the reflection point lies well within the ionospheric layer, as is almost always the case in the high frequency band. The vertical component of $\boldsymbol{\kappa_0}$ has a minimum magnitude such that the thickness of the ionosphere, $2z_0$, is equal to half a wavelength, $\pi/|\kappa_0 l_y|$:

$$2z_0 = \frac{\pi}{|\kappa_0 l_y|}. \tag{46}$$

Rearranging, we have

$$\kappa_0^2 = \left(\frac{\pi}{2z_0 l_y}\right)^2, \tag{47}$$

as desired. We can therefore combine the factors in the denominator of (45):

$$R_{\phi_1}(X,Y)\Big|_{\substack{|X|\ll\kappa_0^{-1}\\ |Y|\ll\kappa_0^{-1},\, z_0}} = \kappa_0|X|K_1(\kappa_0|X|)\int_{-\infty}^{\infty}\frac{4\kappa_0 z_0(r_e\lambda)^2\,\langle n_1^2\rangle\, e^{i\kappa_y Y}\,d\kappa_y}{l_y l_z(\kappa_0^2+\kappa_y^2/l_z^2)^{3/2}}. \tag{48}$$

Using (9.6.25) in [13] we can evaluate the integral:

$$R_{\phi_1}(X,Y)\Big|_{\substack{|X|\ll\kappa_0^{-1}\\ |Y|\ll\kappa_0^{-1},\, z_0}} = \left[\frac{8z_0(r_e\lambda)^2\,\langle n_1^2\rangle}{\kappa_0 l_y}\right]\left[\kappa_0|X|K_1(\kappa_0|X|)\right]\left[\kappa_0 l_z|Y|K_1(\kappa_0 l_z|Y|)\right]. \tag{49}$$

Brackets have been inserted for the purpose of interpretation. The first bracketed factor is the mean-square phase, and the second and third bracketed factors are the X and Y dependencies that both go to unity at $X = 0$ and $Y = 0$, respectively.

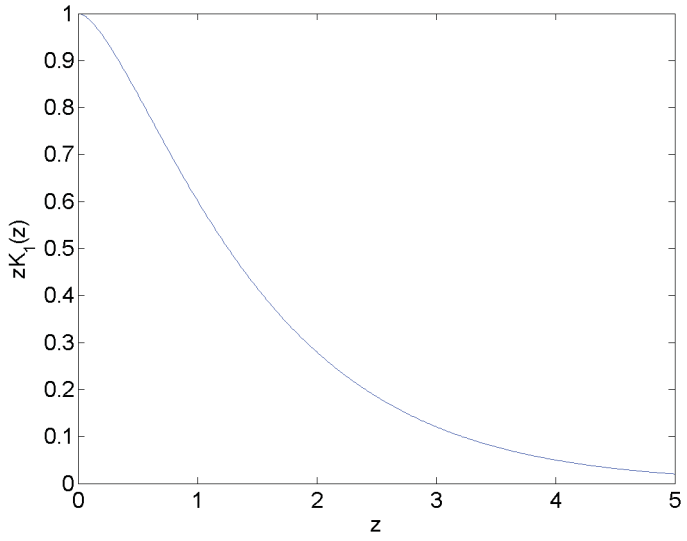

Figure 2: *The function* $zK_1(z)$.

To get a better intuitive picture of $R_{\phi_1}(X,Y)$ we plot the function $zK_1(z)$ in Figure 2. The function drops to one-half at approximately $z = 1$. In (49), the corresponding half-power widths are κ_0^{-1} in the X direction and $(\kappa_0 l_z)^{-1}$ in the Y direction. However, the condition $|X|, |Y| \ll \kappa_0^{-1}, z_0$ means that the phase autocorrelation (49) agrees with Figure 2 only for $z \ll 1$. In the next section it is shown that this is not a serious limitation of the theory, as it turns out that the complex amplitude autocorrelation only depends on the behaviour near the peak.

Finally, we compare the new result (49) with the conventional result based on (32). By carrying out the inverse transforms on (32), the reader can prove as an exercise that the conventional autocorrelation is given by

$$R_{\phi_1}(X,Y) = \left[\frac{8z_0(r_e\lambda)^2\,\langle n_1^2\rangle}{\kappa_0 l_y}\right]\left[\kappa_0|X|K_1(\kappa_0|X|)\right]. \tag{50}$$

The mean-square phase in the conventional expression is the same as in the new expression (49). However, there is no Y dependence, meaning that the phase is perfectly correlated in the Y direction. In contrast, the new theory predicts finite Y correlation, with an axial ratio (the ratio of correlation lengths in Y and X) given by l_z^{-1}. This is the secant of the magnetic field angle with respect to the vertical direction.

In the next section we will derive the complex amplitude autocorrelation. It will be shown that the small argument approximation used above for the phase autocorrelation is sufficient for the computation of the complex amplitude autocorrelation.

3.3 Complex amplitude autocorrelation

Signal phase cannot be measured directly with radio receivers. What receivers measure is the signal complex amplitude $a_1 = e^{i\phi_1}$. However, phase outside the interval $(-\pi, \pi)$ is ambiguous when represented as a complex amplitude. This means that the complex amplitude must be treated in its own right. The correlation function of the complex amplitude R_{a_1} is related to the correlation function of the phase R_{ϕ_1} by [14]

$$R_{a_1}(X,Y) = e^{R_{\phi_1}(X,Y) - R_{\phi_1}(0,0)} = e^{R_{\phi_1}(0,0)\left[\kappa_0|X|K_1\left(\kappa_0|X|\right)\kappa_0 l_z|Y|K_1\left(\kappa_0 l_z|Y|\right) - 1\right]}, \qquad (51)$$

where $R_{\phi_1}(0,0)$ is the mean-square phase fluctuation, given by the first bracketed factor in (49). If we consider the example $z_0 \approx \kappa_0^{-1} \approx 5 \times 10^4$ m, $l_y \approx 0.5$, $r_e \approx 2.8 \times 10^{-15}$ m, $\lambda \approx 100$ m (3 MHz operation), $\langle n_1^2 \rangle \approx 10^{18}$ m^{-6} (1% density fluctuations), then

$$R_{\phi_1}(0,0) = \frac{8 z_0 (r_e \lambda)^2 \langle n_1^2 \rangle}{\kappa_0 l_y} \approx 3000. \qquad (52)$$

The mean-square phase is clearly much greater than unity. In (51), this mean-square phase multiplies functions of the form $zK_1(z)$, which have width $|z| \approx 1$. Therefore R_{a_1} has widths $|X| \ll \kappa_0^{-1}$ and $|Y| \ll (l_z \kappa_0)^{-1}$. Since these were precisely the conditions that were imposed on R_{ϕ_1}, the expression for R_{a_1} above can be written without conditions on the size of X and Y. Finally, to illustrate the shape of R_{a_1}, we plot the function $e^{\alpha[zK_1(z)-1]}$ in Figure 3, with $\alpha = 3000$. A small-argument expansion of $K_1(z)$ [13] will show the width of R_{a_1} to be on the order of $\alpha^{-1/2}$.

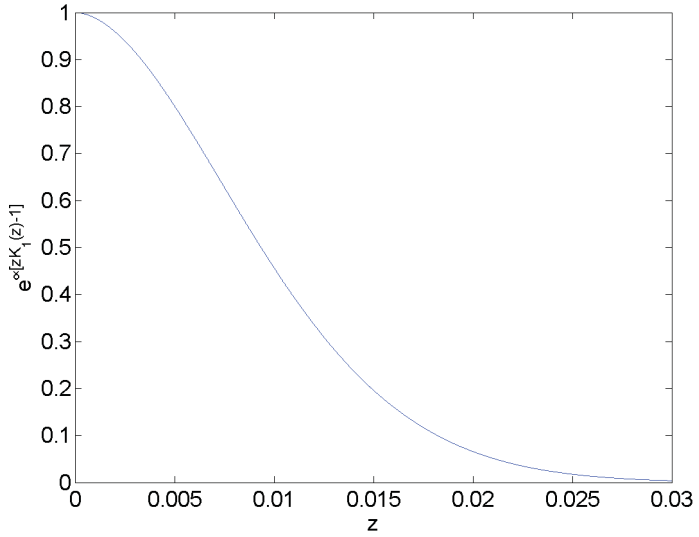

Figure 3: *The function* $e^{\alpha[zK_1(z)-1]}$ *with* $\alpha = 3000$.

4 Conclusion

This memorandum has presented a revised theory for the prediction of the spatial autocorrelation function of an HF radar echo from the ionosphere. The autocorrelation (51) has a number of interesting features that help explain observations of ionospheric echoes. First, the axial ratio, namely the ratio of the correlation lengths in the Y (magnetic north-south) and X (magnetic east-west) directions is no longer infinite, but rather it is equal to l_z^{-1}. This is the secant of the angle of the magnetic field with respect to vertical. More commonly, one speaks of the magnetic dip angle with respect to horizontal, in which case the axial ratio is equal to the cosecant of the dip angle. It is only at the magnetic equator (zero dip angle) where the predicted axial ratio goes to infinity.

The second feature of the provided theory is that the X and Y dependencies of the complex amplitude autocorrelation are both of the form of the function $zK_1(z)$. The derivative of this function approaches zero as $z \to 0$, as can be seen in Figure 3, and can be verified by small-argument expansions. This means that the autocorrelation takes on a Gaussian-like appearance. This is favourable for adaptive clutter suppression with multi-dimensional arrays since the correlation function is nearly flat for the short distances typical of fully sampled radar apertures.

The third feature of the theory is that there is a prediction for the mean-square phase fluctuation (52) that is based on physically meaningful parameters, such as density fluctuation mean-square amplitude at the reflection height. This is in contrast to the conventional theory, where the density fluctuation is only loosely defined as a volume average.

These improvements should lead to higher fidelity models for predicting adaptive array processing performance. Similar ideas could also be applied to the case of oblique (non-vertical incidence) propagation, although the mathematics would be more complicated since the wave packet trajectory is no longer rotationally symmetric around a vertical axis.

References

[1] Sevgi, L., Ponsford, A. M., Chan, H. C. (2001). An integrated maritime surveillance system based on high-frequency surface-wave radars, part 1: Theoretical background and numerical simulations. *IEEE Antennas and Propagation Magazine*, 43 (4), 28–43.

[2] Budden, K. G. (1985). The propagation of radio waves: The theory of radio waves of low power in the ionosphere and magnetosphere. Cambridge, UK: Cambridge University Press.

[3] Abramovich, Y., Anderson, S., Lyudviga, Y., Spencer, N., Turcaj, P., and Hibble, B. (2004). Space-time adaptive techniques for ionospheric clutter mitigation in HF surface wave radar systems, In *Proceedings of the 2004 International Conference on Radar Systems*, Toulouse, France.

[4] Riddolls, R. J., Adve, R. S. (2009). Two-dimensional adaptive processing for ionospheric clutter mitigation in high frequency surface wave radar, In *Proceedings of the 2009 IEEE radar conference*, Pasadena, California, USA.

[5] Basler, R. P., Price, G. H., Tsunoda, R. T., and Wong, T. L. (1988). Ionospheric distortion of HF signals. *Radio Science*, 23 (4), 569–579.

[6] Coleman, C. J. (1996). A model of HF sky wave radar clutter. *Radio Science*, 31 (4), 869–875.

[7] Tatarskii, V. I. (1961). Wave propagation in a turbulent medium. New York: Dover.

[8] Rufenach, C. L. (1975). Ionospheric scintillation by a random phase screen: Spectral approach. *Radio Science*, 10 (2), 155–165.

[9] Chen, F. F. (1984). Introduction to plasma physics and controlled fusion. 2nd ed. New York: Plenum Press.

[10] Kelley, M. C. (1989). The earth's ionosphere. San Diego: Academic Press.

[11] Woodman, R. F. and Basu, S. (1978). Comparison between in situ measurements of F-region irregularities and backscatter observations at 3-m wavelength. *Geophysical Research Letters*, 5, 869–872.

[12] Vallieres, X., Villain, J.-P., Hanuise, C., Andre, R. (2004). Ionospheric propagation effects on spectral widths measured by SuperDARN HF radars. *Annales Geophysicae*, 22, 2023–2031.

[13] Abramowitz, M. and Stegun, I. A. (1964). Handbook of mathematical functions with formulas, graphs, and mathematical tables. New York: Dover.

[14] Reed, I. S. (1962). On a moment theorem for complex Gaussian processes. *IRE Transactions on Information Theory*, 8 (4), 194–195.

This page intentionally left blank.

DOCUMENT CONTROL DATA

(Security classification of title, body of abstract and indexing annotation must be entered when the overall document is classified)

1. ORIGINATOR (the name and address of the organization preparing the document. Organizations for whom the document was prepared, e.g. Establishment sponsoring a contractor's report, or tasking agency, are entered in section 8.)

   Defence R&D Canada - Ottawa
   Ottawa ON K1A 0Z4

2. SECURITY CLASSIFICATION (overall security classification of the document, including special warning terms if applicable)

   UNCLASSIFIED
   (NON-CONTROLLED GOODS)
   DMC A
   REVIEW: GCEC June 2010

3. TITLE (the complete document title as indicated on the title page. Its classification should be indicated by the appropriate abbreviation (S,C or U) in parentheses after the title.)

   Modification of a high frequency radar echo spatial correlation function by propagation in a linear plasma density profile (U)

4. AUTHORS (Last name, first name, middle initial)

   Riddolls, Ryan, J.

5. DATE OF PUBLICATION (month and year of publication of document)

   December 2011

6a. NO. OF PAGES (total containing information. Include Annexes, Appendices, etc.)

   26

6b. NO. OF REFS (total cited in document)

   14

7. DESCRIPTIVE NOTES (the category of the document, e.g. technical report, technical note or memorandum. If appropriate, enter the type of report, e.g. interim, progress, summary, annual or final. Give the inclusive dates when a specific reporting period is covered.)

   Technical Memorandum

8. SPONSORING ACTIVITY (the name of the department project office or laboratory sponsoring the research and development. Include the address.)

   Defence R&D Canada - Ottawa
   Ottawa ON K1A 0Z4

9a. PROJECT OR GRANT NO. (if appropriate, the applicable research and development project or grant number under which the document was written. Please specify whether project or grant)

   Project 11hj01

9b. CONTRACT NO. (if appropriate, the applicable number under which the document was written)

10a. ORIGINATOR'S DOCUMENT NUMBER (the official document number by which the document is identified by the originating activity. This number must be unique to this document.)

   DRDC Ottawa TM 2011-219

10b. OTHER DOCUMENT NOS. (Any other numbers which may be assigned this document either by the originator or by the sponsor)

11. DOCUMENT AVAILABILITY (any limitations on further dissemination of the document, other than those imposed by security classification)

   (X) Unlimited distribution
   ( ) Distribution limited to defence departments and defence contractors; further distribution only as approved
   ( ) Distribution limited to defence departments and Canadian defence contractors; further distribution only as approved
   ( ) Distribution limited to government departments and agencies; further distribution only as approved
   ( ) Distribution limited to defence departments; further distribution only as approved
   ( ) Other (please specify):

12. DOCUMENT ANNOUNCEMENT (any limitation to the bibliographic announcement of this document. This will normally correspond to the Document Availability (11). However, where further distribution (beyond the audience specified in 11) is possible, a wider announcement audience may be selected.)

   Unlimited

13. ABSTRACT (a brief and factual summary of the document. It may also appear elsewhere in the body of the document itself. It is highly desirable that the abstract of classified documents be unclassified. Each paragraph of the abstract shall begin with an indication of the security classification of the information in the paragraph (unless the document itself is unclassified) represented as (S), (C), or (U). It is not necessary to include here abstracts in both official languages unless the text is bilingual).

This memorandum examines the spatial autocorrelation function for echoes from an ionospheric plasma in the High Frequency (HF) range. Conventional treatments of this problem assume that the amount of signal phase shift for a given plasma density fluctuation in the ionospheric propagation medium remains constant along the propagation path. For HF radar signal propagation through an ionospheric plasma with field-aligned density structures, the phase autocorrelation is predicted to be highly anisotropic, with essentially perfect correlation in the magnetic north-south direction. In this memorandum a revised theory is provided that accounts for a spatial-dependent derivative of signal wavenumber with respect to plasma density in an ionosphere with a linear plasma density profile. This revised theory leads to a prediction of a far more isotropic autocorrelation, with an axial ratio equal to the cosecant of the local magnetic dip angle. This theory provides a more realistic basis for predicting the performance of spatial adaptive antenna arrays for the rejection of vertical incidence ionospheric clutter in HF Surface Wave Radar (HFSWR) systems.

14. KEYWORDS, DESCRIPTORS or IDENTIFIERS (technically meaningful terms or short phrases that characterize a document and could be helpful in cataloguing the document. They should be selected so that no security classification is required. Identifiers such as equipment model designation, trade name, military project code name, geographic location may also be included. If possible keywords should be selected from a published thesaurus. e.g. Thesaurus of Engineering and Scientific Terms (TEST) and that thesaurus-identified. If it is not possible to select indexing terms which are Unclassified, the classification of each should be indicated as with the title.)

High Frequency
Radar
Radio
Scattering
Clutter
Correlation
Spectrum

Defence R&D Canada

Canada's leader in Defence
and National Security
Science and Technology

R & D pour la défense Canada

Chef de file au Canada en matière
de science et de technologie pour
la défense et la sécurité nationale

www.drdc-rddc.gc.ca